3-D Printing of Elements in Frequency Selective Arrays

Benito Sanz-Izquierdo and Edward A. Parker

***Abstract*—3-D printing is a technology that enables the fabrication of complex objects directly from a digital model. Folding the elements of Frequency Selective arrays in three dimensions gives a significant reduction in the resonant frequency for a given cell dimension, and such structures are candidates for additive manufacture. The aim in this paper is to demonstrate by example the development of novel electromagnetic structures that could be fabricated in parallel and integral with the additive manufacture of buildings, for electromagnetic architecture control. The principle is illustrated with two new geometries based on dipole and loop elements. The cores of these structures were fabricated with a 3-D printer that uses a plaster-based material. Theoretical and experimental results confirm the operation of the surfaces within the UHF frequency band.**

***Index Terms*—3-D printing, Additive manufacture, electromagnetic architecture, electromagnetic wave propagation, frequency selective surfaces.**

I. Introduction

ADDITIVE manufacturing or 3-D printing is a technology that enables the fabrication of complex objects directly from a digital model. Three-dimensional printing is achieved by laying down successive layers, each of slightly different shape. This technology has been evolving quite rapidly in recent years and is nowadays seen an alternative to traditional manufacturing methods. Potential applications of 3-D printing have expanded from its origins in the fabrication of mechanical objects to the incorporation of electrical circuits in the manufacturing process [1]–[4]. The popularity of this technology has reached the built environment, where architects have recently proposed buildings fully fabricated using 3-D printers [5]. As part of this construction process, 3-D printed building blocks could incorporate frequency selective structures into the Electromagnetic Architecture, to control electromagnetic wave propagation within buildings [6]–[8].

Frequency selective surfaces (FSS) are typically two-dimensional periodic structures that filter electromagnetic waves over a range of frequencies. Expansion into a volume [9]–[13] or extension to a three dimensional profile [14] creates a 3-D frequency selective structure. Some volumetric FSS such as those based on the caltrop offer higher stability to angle of illumination than their corresponding 2-D FSS, the tripole, when placed on a regular lattice [10]. Similarly, in [11], [12], placing multimode cavities on a two-dimensional lattice was demonstrated to exhibit superior performance over traditional FSS. Another recent development in [13], has achieved wide frequency response by connecting two cascaded radiating elements.

This paper presents 3-D frequency selective structures whose elements are fabricated using additive manufacturing techniques. Three-dimensional printing the FSS elements creates relatively light weight structures that could be readily placed in walls in a building. A new concept of folding FSS elements in three dimensions is introduced with two different elements as an illustration. Section II describes the process of 3-D folding a singly polarized dipole element and analyses its performance. Section III looks at the implementation of the technique to dual-polarized FSS with the use of a loop element. The behavior of the surfaces including the effect of folding on resonance frequency and angular stability are described. Simulations using CST Microwave Studio are compared with experiments, and the results are discussed. The paper closes with concluding remarks that summarize the design and measurements.

II. 3-D Folded Dipole

A. Design and Analysis

Periodic arrays of dipole elements are among the simplest configurations that can be used as frequency selective surfaces. As with more complex FSS, they transmit at a certain frequency and reflect at others. One limitation of this element is the relatively large lattice unit cell in relation to the resonant wavelength. Convoluting the slots or the conductors of FSS elements has been demonstrated to produce a major reduction in the resonant frequency and in the sensitivity of the reflection/transmission band to angle of incidence [15]–[19].

The simplest level of convolution is the addition of a single stub [20] to the dipole structure as shown in Fig. 1(a). This planar element has here been extended out of the plane to create a 3-D pattern that could be fabricated while maintaining sufficient mechanical strength. The depth of the stub was increased as in Fig. 1(b) and folded to create the structure in Fig. 2. Top view and side views of the structure are shown in Fig. 1(c) and (d), respectively. The 2-D unit cell has the same

Manuscript received July 24, 2013; revised February 07, 2014; accepted August 09, 2014. Date of publication September 19, 2014; date of current version November 25, 2014. This project was funded by a research grant from the Faculty of Sciences at the University of Kent, the UK EPSRC and the UK Royal Society.

The authors are with the School of Engineering and Digital Arts, University of Kent, Canterbury, CT2 7NT, U.K. (e-mail: b.sanz@kent.ac.uk, e.a.parker@kent.ac.uk).

Color versions of one or more of the figures in this paper are available online at http://ieeexplore.ieee.org.

Digital Object Identifier 10.1109/TAP.2014.2359470

0018-926X © 2014 IEEE. Translations and content mining are permitted for academic research only. Personal use is also permitted, but republication/redistribution requires IEEE permission. See http://www.ieee.org/publications_standards/publications/rights/index.html for more information.

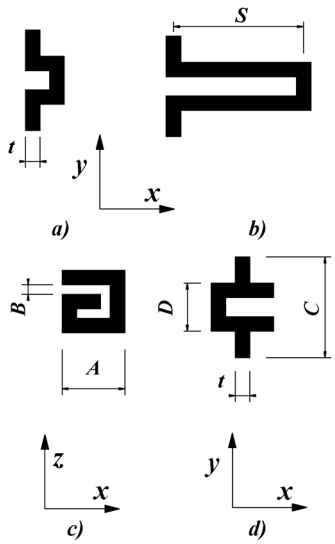

Fig. 1. Development of a 3-D folded dipole element: (a) initial structure; (b) the element with an extended stub; (c) upper view of the 3-D element; (d) side view.

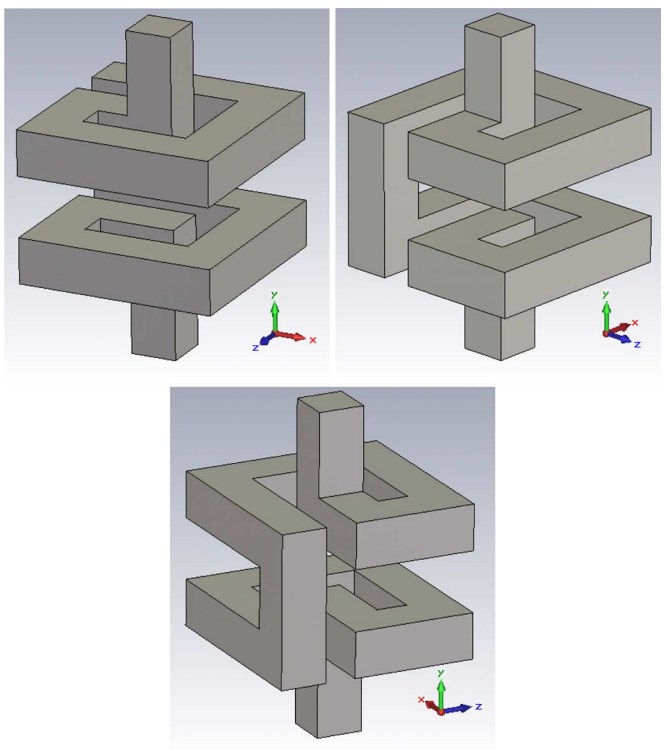

Fig. 2. Three different views of the 3-D folded dipole element.

size as that for the initial structure but it is able to accommodate a longer conductor, as with all convoluted elements. An illustrative design was computed with the following dimensions: $A = 13$ mm, $B = 2$ mm, $C = 21$ mm, and $D = 10$ mm (see Fig. 1(c) and (d)). The thickness $t = 3$ mm was maintained in the whole structure to keep mechanical strength. The element was placed in a square unit cell of length $p = 26$ mm along the xy plane. The design was simulated as a loosely packed infinite array using the periodic unit cell template included in CST Microwave Studio.

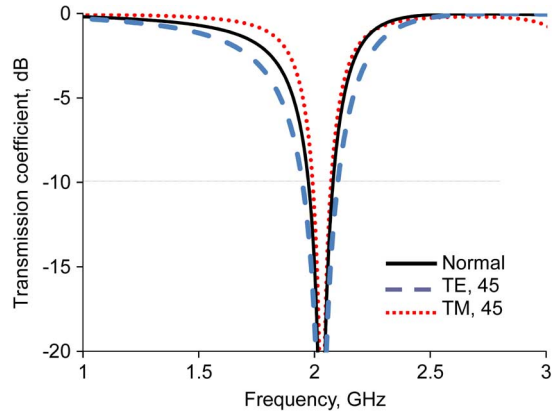

Fig. 3. Simulated transmission responses of the 3-D folded dipole FSS, E vector parallel to the y axis.

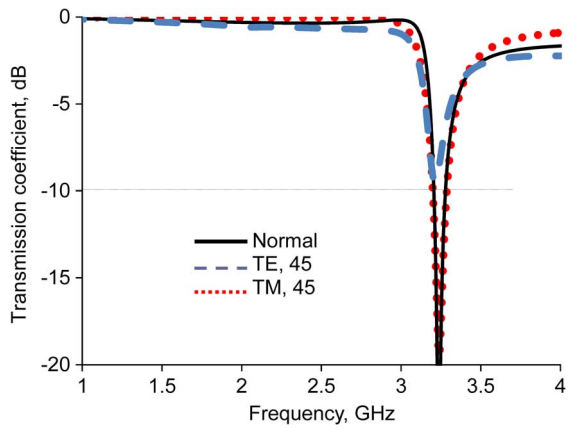

Fig. 4. Simulated transmission responses of the 3-D folded dipole FSS, E vector parallel to the x axis.

Fig. 3 shows the transmission responses when the incident E vector of the plane wave was parallel to the y axis. Resonance occurred for a unit cell size of $(0.16\lambda_r)^2$ at normal incidence with no appreciable frequency drift at TE45 and TM45 (i.e. illumination at 45 degrees off broadside for TE and TM polarization). The figure of merit as defined by λ_r/p in [15] was about 6, while the ratio L/λ_r was 0.6. λ_r is the wavelength at resonance. L is the total length of the conductor.

When the incident E-field was parallel to the x axis (Fig. 4), the FSS resonated for a unit cell size of $(0.25\lambda_r)^2$, with no clear change at TE45 and TM45.

B. Parametric Analysis

As pointed out in [18], the resonant frequency and bandwidth of an FSS is influenced by the thickness of the elements, particularly if their shapes are convoluted. The thinner the element, the lower the resonant frequency and the higher the figure of merit λ_r/p. Fig. 5 shows the effect of varying the thickness t of the loaded dipole element (Fig. 1(a)) on λ_r/p at normal incidence, TE45 and TM45. Experiments with the Z650 printer from ZCorp, indicated that the minimum thickness to give sufficient mechanical strength was $t = 3$ mm. This thickness allows for fabrication using most commercial 3-D printers. The corresponding figure of merit $(\lambda_r/p = 2)$ is low, but still better than the one reported in [15] for loaded dipole slots $(\lambda_r/p = 1.5)$.

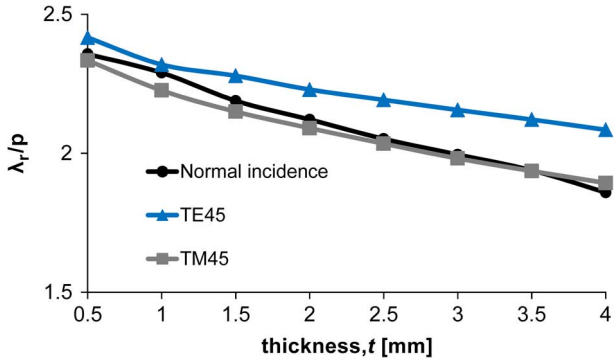

Fig. 5. Figure of merit λ_r/p dependence on element thickness t of the loaded dipole in Fig. 1(a).

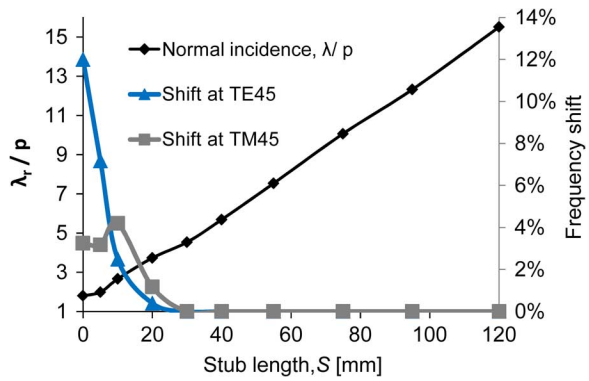

Fig. 6. Computed effect of folding the dipole FSS element: λ_r/p at normal incidence, and frequency shift at TE45 and TM45.

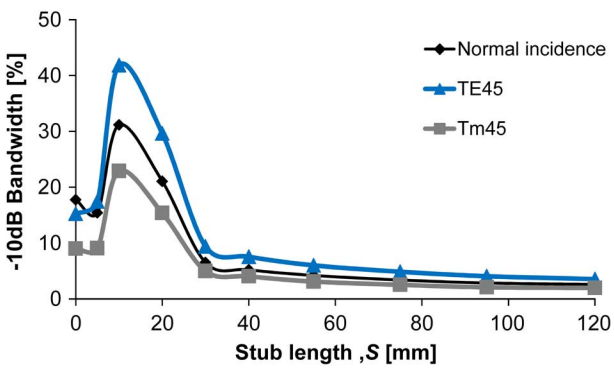

Fig. 7. Computed effect of folding the structure on −10-dB bandwidth at normal incidence, TE45 and TM45.

The effect of 3-D folding on λ_r/p is shown in Fig. 6. Starting from a simple dipole element, the length of the stub, S [Fig. 1(b)], was increased and folded [Fig. 1(c)]. It can be observed that, at normal incident angle, the simple dipole resonated at almost 8 times the frequency of the fully convoluted structure. The sensitivity to angle of incidence improved significantly from 0 to 20 mm, and there was almost no shift from 40 mm onwards. The 10-dB bandwidth of the structure (Fig. 7) increased for stub lengths from 0 to 10 mm, decreased rapidly from 10 mm to 30 mm, and decreased at a slower rate between 30 mm to 120 mm. Note that the element fabricated and measured in this paper (Fig. 2) corresponds to a stub length of $S = 40$ mm.

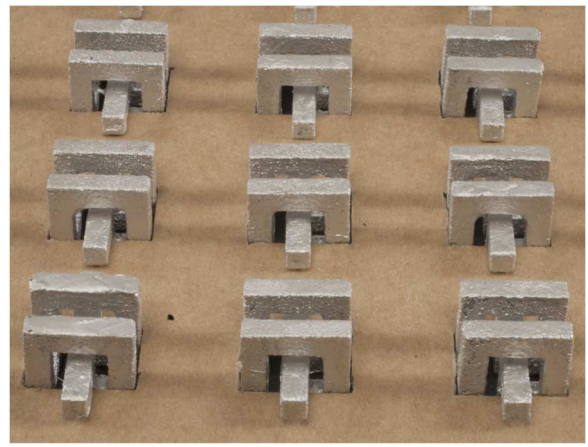

Fig. 8. Photograph of 3 ×3 elements of the 3-D folded dipole element.

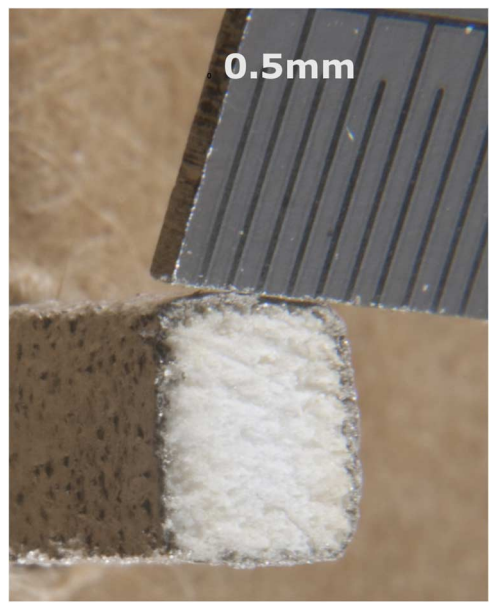

Fig. 9. Cross-sectional cut of one of the elements.

C. Fabrication and Measurements

The digital design from CST Microwave Studio was exported on a stereographic (.stl) file and then transferred to a 3-D Z650 printer from ZCorp for fabrication. The material used by this device has a trade name zp150 [21] which consists mainly of a plaster material, with the addition of a vinyl polymer and a carbohydrate. Two coating layers of silver were then, in this illustration, applied by hand. The averaged measured conductivity was approximately 2×10^6 S/m. A 9 ×9 frequency selective array was then created by placing the elements in apertures that were laser cut into a fiberboard support approximately 2 mm thick to ensure sufficient mechanical strength, and which had internal corrugations with air gaps for low permittivity and dielectric losses. A 3 ×3 array of the final structure is shown in Fig. 8. A cross-sectional cut of the structure is shown in Fig. 9, and a microscopic view of the typical surface contour is in Fig. 10. The Keyence VHX2000 Digital Microscope with the VH-Z100 Lens was used for the magnification. Surface roughness and nonuniformity of the applied layer of silver conductive paint

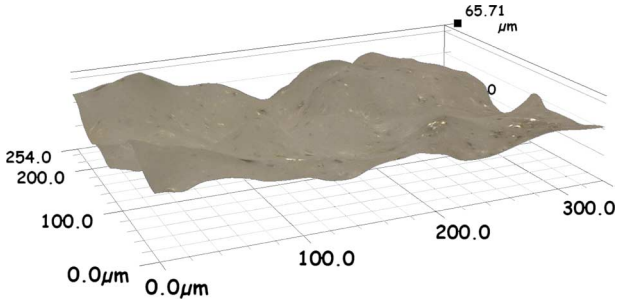

Fig. 10. Microscopic view of the typical surface contour of the structure.

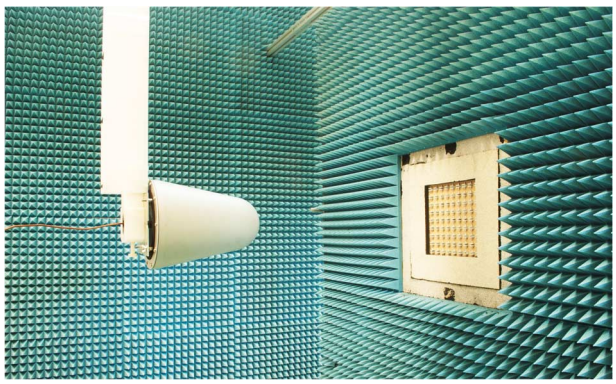

Fig. 11. Absorbing panel with the FSS in the test chamber.

can be seen. In this particular, case the rms deviation from the mean surface was approximately 10 μm.

The measurement set up consisted of a test chamber equally divided by a microwave absorber loaded rotatable screen, thus allowing for angle of incidence transmission measurements. The screen had a centrally located adjustable aperture that accepts the surface under test. A photograph showing the transmitted antenna and the panel containing the FSS is shown in Fig. 11. The system was calibrated relative to an aperture of approximately 250 mm $\times$250 mm in the center of the panel. The responses of the FSS set perpendicularly to the axis of the antennas, and at 45 ° (nominally TE45 and TM45) with the incident E vector in the yz plane [Fig. 1(d)] are shown in Fig. 12. In all three cases, the FSS resonated at about 2GHz and, when E field was in the xz plane, it resonated at 3.2 GHz at normal incidence with no significant drift at TE45 and TM45 (Fig. 13). Despite the relatively low resolution of the fabrication techniques used, the resistance of the silver conductive layers, particle–particle disconnects and the roughness of the surfaces (Fig. 10), these frequencies agreed well with those in the simulations (Figs. 3 and 4). The use of thick components improves the tolerance to these factors, and is very suited to the standards expected in the fabrication of buildings.

III. 3-D Folded Loop Element

A. Design and Analysis

Loop FSS are dual polarized structures with simple transmission frequency response, in the patch version consisting of a reflection resonance, with a transmission band at low frequencies. They resonate when the circumference is close to λ_r, leading to

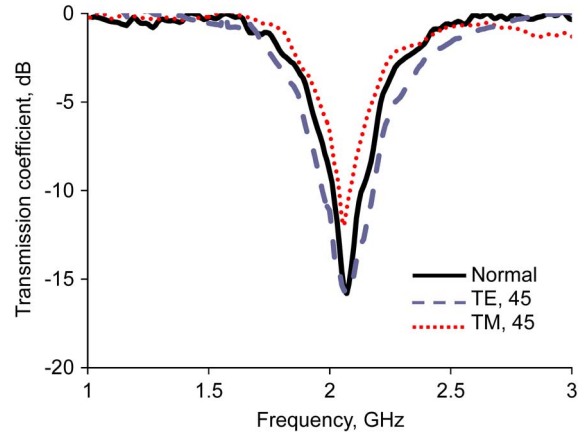

Fig. 12. Measured transmission response of the 3-D folded dipole element at normal incidence, TE45 and TM45, E vector parallel to the y axis.

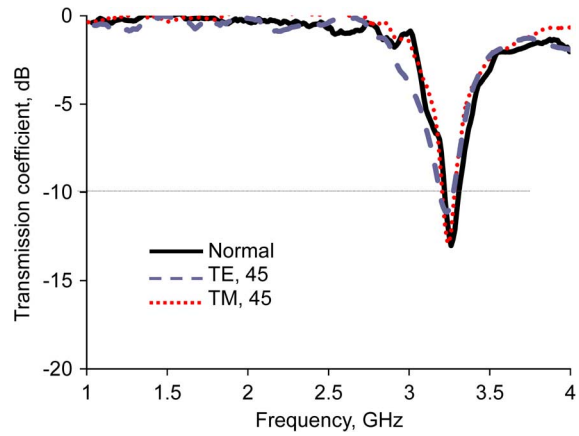

Fig. 13. Measured transmission response of the 3-D folded dipole element at normal incidence, TE45 and TM45, E vector parallel to the x axis.

a relatively compact design [22]–[24]. The "four-legged loaded element" is a loop that can be developed from a dipole loaded with a stub [25]. Its figure of merit was reported in [16] to be about $\lambda_r/p = 2.2$. This configuration was used to create a dual-polarized 3-D folded FSS, as a second illustration. The resulting structure is shown in Fig. 14. As can be seen from the figure, the legs have been folded to the back of the structure using the same procedure as that described for the dipole FSS. This new design was tuned to the 2.5 GHz wireless LAN frequency band, resulting in the dimensions in Fig. 15, where: $h = 35$ mm, $w = 9$ mm, $d = 10$ mm, $f = 4$ mm, $b = 3$ mm, $c = 8.5$ mm, and $t = 3$ mm. The element was arranged on a square lattice with a 36-mm periodicity, giving a tightly packed array.

Simulated transmission responses of an infinite array of these elements are shown in Fig. 16. The FSS resonated at a unit cell size of about $(0.3\lambda_r)^2$ with a 3% frequency shift at TE45 and less than 1% shift at TM45. This corresponds to a figure of merit [16] $\lambda_r/p = 3$ and $L/\lambda_r = 1.8$. As discussed in Section II-B, performance could be further improved by decreasing the thickness of the element. For example, if t could be reduced to 0.5 mm, the FSS would resonate at a unit cell size of $(0.19\lambda_r)^2$ with a frequency shift of less than 0.5% at both TE45 and TM45. The figure of merit would increase to about $\lambda_r/p = 5$ and the efficiency of the wire would improve to $L/\lambda_r = 1.2$.

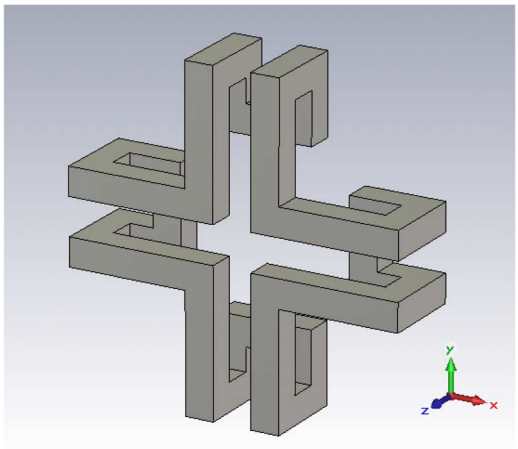

Fig. 14. 3-D folded loop element.

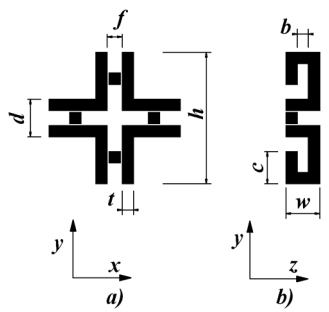

Fig. 15. (a) Front and (b) side views of the 3-D folded loop element.

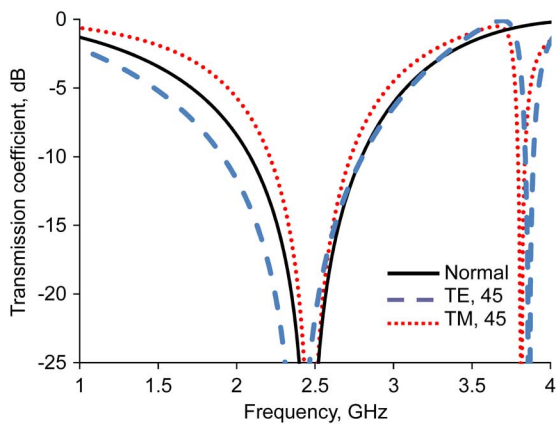

Fig. 16. Simulated transmission responses of the 3-D folded loop FSS.

B. Parametric Analysis

A study of the effect of folding the structure on the resonant frequency and bandwidth of the transmission curves was carried out and is presented in Figs. 17–20. The parameters c and w were varied independently in order to assess their contribution to resonance. Varying c from 3 to 6 mm (Fig. 17) did not affect significantly the resonant frequency and bandwidth. From 6 mm to 12 mm, however, the resonant frequency decreased by 20% and the bandwidth by about 10%.

In order to assess the effect of w, c was set equal to the thickness t (3 mm), i.e., with no folding along the y axis. As can be

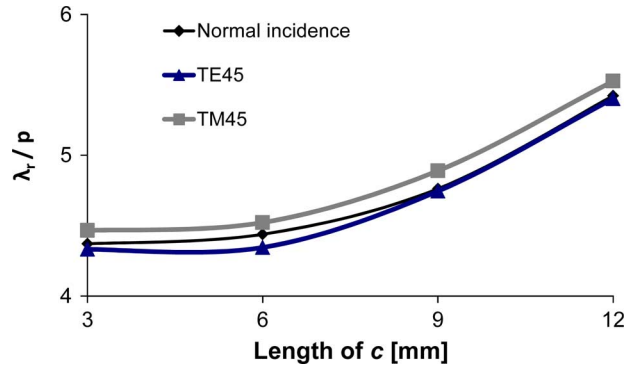

Fig. 17. Computed effect of varying c (Fig. 15) on λ_r/p at normal incidence, TE45 and TM45.

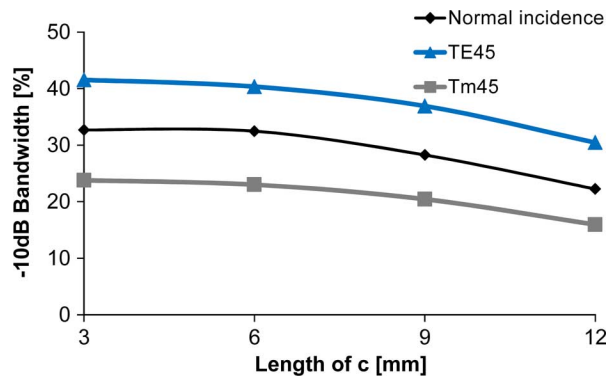

Fig. 18. Computed effect on −10-dB bandwidth at normal incidence, TE45 and TM45 of varying c (Fig. 15).

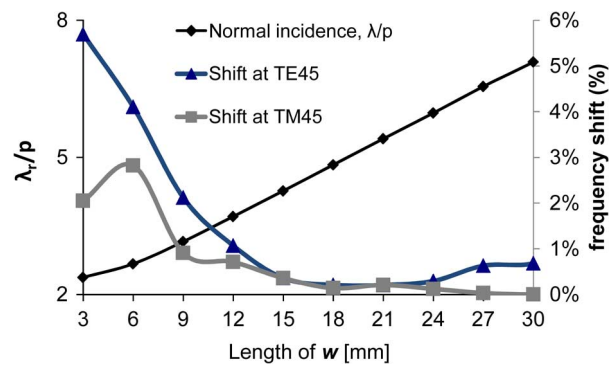

Fig. 19. Computed effect of varying w (Fig. 15) on λ_r/p at normal incidence, TE45 and TM45.

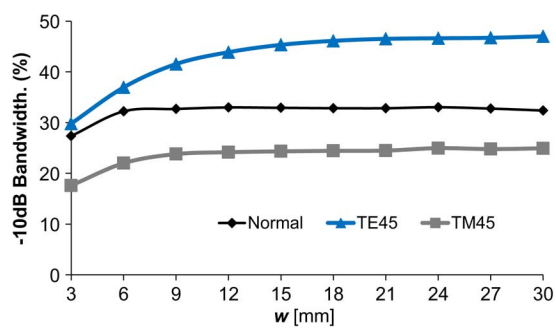

Fig. 20. Computed effect on −10-dB bandwidth at normal incidence, TE45 and TM45 of varying w (Fig. 15).

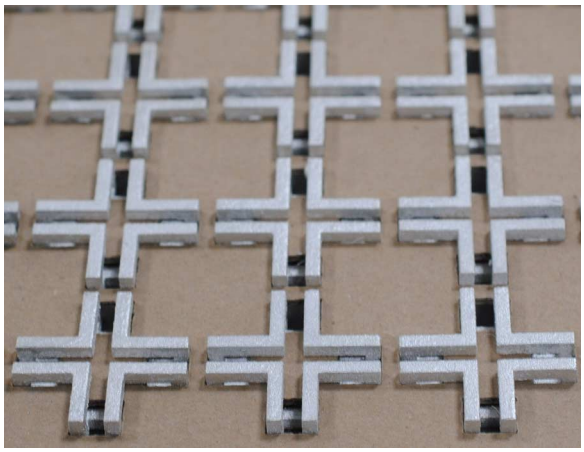

Fig. 21. A 3 × 3 array of the 3-D folded loop FSS.

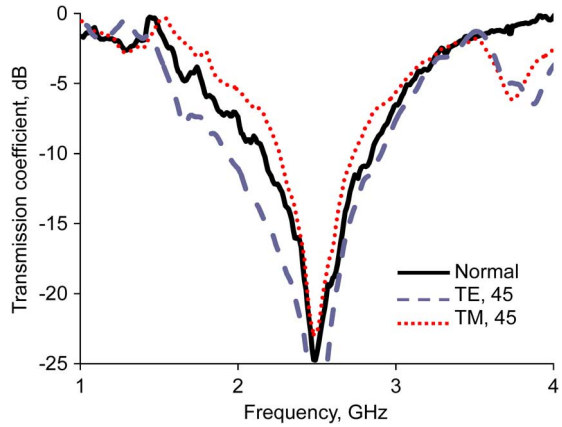

Fig. 22. Measured transmission responses of the 3-D folded loop.

seen from Fig. 19, extending the structure in the z axis increases the ratio λ_r/p linearly following the equation

$$\frac{\lambda_r}{p} = 0.1835w + 1.582. \quad (1)$$

This linear behavior might be expected, as the length of the conductor has been increased. Furthermore, large computed values of w fitted well the equation. For example, CST calculations for $w = 93$ mm was only 0.02% lower than the one obtained using (1).

The −10-dB bandwidth at normal incidence increased from 3 mm to 6 mm but then remain constant at about 32%. At TE45 and TM45, the bandwidth increased rapidly from 3 mm to 9 mm and then continue increasing at a lower rate. At $w = 93$ mm, for example, the bandwidths were 32.7%, 49.8% and 26.9% at normal incidence, TE45 and TM45, respectively.

C. Fabrication and Measurements

A 7 ×7 array of the 3-D folded loops in Fig. 14 was manufactured in similar manner to that described in Section II-C. Twenty-five elements were fabricated using the plaster based 3-D printer Z650 from ZCorp. The printed structures were coated with one layer of silver conductive paint and, in this case, cured at a temperature of 125 °C for 5 minutes. As for the first design, the average measured conductivity was approximately 2×10^6 S/m. The final 7 ×7 array was again made by laser cutting the shape of the elements on the 2-mm-thick fiberboard material and placing the structures in the apertures created. A photograph of a 3 ×3 element section of the FSS array is shown in Fig. 21.

The measured transmission responses of the FSS at normal incidence, TE45 and TM45 when the incident E vector was in the yz plane (Fig. 14) are shown in Fig. 22. Note that in this figure, the transmitivity has not yet reached its maximum at low frequencies—it would be higher below 1 GHz (compare the simulations in Fig. 16). Grating effects influence the upper frequencies. There is a resonance at about 2.5 GHz. It is deeper than the one obtain for the folded dipole (Fig. 12), reaching 25 dB or more for the three reflection curves. The frequency shifts were about 4% at TE45 and less than 0.5% at TM45. The reflection bandwidths at the −10-dB mark were about 24% at normal incidence, 40% at TE45 and 14% at TM45. In all three cases, the WLAN frequency band was covered by a transmission level below −17 dB. Measurements compared well with the simulations, showing that even a relatively small array of these elements (7 ×7) maintains the reflection characteristics of the infinite FSS [8].

IV. Conclusion and Discussion

This investigation of the potential applicability of the latest 3-D printing technologies to the fabrication of novel frequency selective structures has demonstrated that they can employ materials, plasters, commonly used in the fabrication of internal parts of buildings. That in turn suggests that the incorporation of such structures could become a stage in the sequence of processes undergone during the course of the building process itself, aimed at establishing the specific electromagnetic architecture of a specific building.

Two good examples of the use of 3-D printing to the development of novel frequency selective structures have been presented. These designs were based on the loaded dipole and four legged elements, to which a new folding technique for FSS was applied. 3-D folding the conductors in the way described in this paper is clearly capable of lowering the resonant frequency f_1 while leaving the array periodicity unaltered. Alternatively, the unit cell size needed for operation at a given frequency can be reduced. The stability of the resonant frequency as the angle of wave incidence changes is also improved.

Transmission nulls of over 10 dB in depth were obtained for the folded dipole structure and 25 dB for the folded loop designs. Additionally, the folded loop design was able to cover the 2.4-GHz WLAN band with a reflection level of over 17 dB at normal incidence, TE45 and at TM45. As pointed out in [26], in the built environment relatively small interference attenuation can result in significant improvements in the system outage probability. A 15 dB in carrier-to-interference ratio can reduce the outage probability by a factor of almost 30, and with the inverse square law approximation, just 10 dB reduces the cell separation by a factor of 3, potential enhancements in the efficiency of use of the radio spectrum.

The surface roughness and the thickness of the elements limit its applicability to long wavelengths applications. Other additive manufacturing techniques such as laser sintering

would be ideal for higher frequencies. As the structures were fully coated with conductive paint, most 3-D printing techniques could be employed with equally effective results. The layer of metal could also be added in the printing process. For example, the Z650 printer contains color cartridges that could include metal inks. Large array sizes could be fabricated, and a robotic automatic system could be used to place the elements in their supporting structure (Section II-C) for more commercial applications.

ACKNOWLEDGMENT

The authors would like to thank Dr. J. Batchelor and M. A. Ziai for useful discussions, E. Labrosciano, Kevin. Smith, and M. Samra for their assistance in the fabrication of the 3-D structures, and D. Zala from Keyence for providing the microscopic measurements.

REFERENCES

[1] J. Czyżewskia, P. Burzyńskia, K. Gawełb, and J. Meisnerc, "Rapid prototyping of electrically conductive components using 3D printing technology," *J. Mater. Process. Technol.*, vol. 209, no. 12–13, pp. 5281–5285, Jul. 1, 2009, ISSN 0924-013610.1016/j.jmatprotec.2009.03.015.

[2] M. P. Alonso, E. Malone, F. C. Moon, and H. Lipson, Reprinting the telegraph: Replicating the vail register using multi-materials 3D printing, Cornell.edu. Web., May 30, 2012. [Online]. Available: http://creativemachines.cornell.edu/sites/default/files/SFF09_Alonso.pdf, (Accessed Jun. 2013)

[3] C Gutierrez, R. Salas, G. Hernandez, D. Muse, R. Olivas, E. MacDonald, M. D. Irwin, and R. Wicker, CubeSat fabrication through additive manufacturing and micro-dispensing. [Online]. Available: Www.cosmiacpubs.org. N.p. n.d. Web, Jun. 18, 2012 [Online]. Available: http://www.cosmiacpubs.org/pubs/IMAPS2011_CassieGutierrezUTEP.pdf, (Accessed June 2013)

[4] S. J. Leigh, RJ Bradley, C. P. Purssell, DR Billson, and D. A. Hutchins, "A simple, low-cost conductive composite material for 3D printing of electronic sensors," *PLoS ONE*, vol. 7, no. 11, p. e49365., 2012, 10.1371/journal.pone.0049365 [Online]. Available: http://www.plosone.org/article/info:doi/10.1371/journal.pone.0049365, (Accessed Jun. 2013)

[5] [Online]. Available: http://www.bbc.co.uk/news/technology-21121061.(accessed Jun. 2013)

[6] M Philippakis, C. Martel, D. Kemp, R. Allan, M. Clift, S. Massey, S. Appleton, W. Damerell, C. Burton, and E. A. Parker, "Application of FSS structures to selectively control the propagation of signals into and out of buildings," Ofcom ref. AY4464A, 2004 [Online]. Available: http://stakeholders.ofcom.org.uk/binaries/research/spectrum-research/exec_summary.pdf

[7] M. Hook and K. Ward, "A project to demonstrate the ability of frequency selective surfaces and structures to enhance the spectral efficiency of radio systems when used within buildings," Ofcom ref. AY4462A, 2004.

[8] E. A. Parker, J. B. Robertson, B. Sanz-Izquierdo, and J. C. Batchelor, "Minimal size FSS for long wavelength operation," *Electron. Lett.*, vol. 44, no. 6, pp. 394–395, Mar. 2008.

[9] S. N. Azemi and W. S.T. Rowe, "3D frequency selective surfaces," *Progress Electromagn. Res. C*, vol. 29, pp. 191–203, 2012.

[10] L. Musa, P. W. B. Au, E. A. Parker, and R. J. Langley, "Sensitivity of tripole and calthrop FSS reflection bands to angle of incidence," *Electron. Lett.*, vol. 25, no. 4, pp. 284–285, 1988.

[11] K. Rashid and Z. Shen, "Three-dimensional monolithic frequency selective structure with dielectric loading," in *Proc. Asia-Pacific Microw. Conf. (APMC)*, 2010, pp. 873–876.

[12] A. K. Rashid and Z. Shen, "Three-dimensional monolithic frequency selective surfaces," in *Proc. Int. Conf. Commun. Circuits, Syst. (ICCCAS)*, 2010.

[13] R. Mittra and C. Pelletti, "Three-dimensional FSS elements with wide frequency and angular responses," in *APS URSI Symp.*, Chicago, IL, USA, Jul. 2012, pp. 1–2.

[14] I. M. Ehrenberg, S. E. Sarma, and B.-I. Wu, "Fully conformal FSS via rapid 3D prototyping," in *Proc. IEEE APS URSI Symp.*, 2012, pp. 1–2.

[15] E. A. Parker and A. N. A. El Sheikh, "Convoluted array elements and reduced size unit cells for frequency-selective surfaces," *IEE Proc. H: Microw., Antennas, Propag.*, vol. 138, pp. 19–22, Feb. 1991.

[16] E. A. Parker, A. N. A. El Sheikh, and A. C. Lima, "Convoluted frequency-selective array elements derived from linear and crossed dipoles," *IEE Proc. H*, vol. 40, no. 5, pp. 378–380, 1993.

[17] E. A. Parker and A. N. A El Sheikh, "Convoluted dipole array elements," *IEE Electron. Lett.*, vol. 27, no. 4, pp. 322–323, 1991.

[18] B. Sanz-Izquierdo, E. A. Parker, J.-B. Robertson, and J. C. Batchelor, "Singly and dual polarized convoluted frequency selective structures," *IEEE Trans. Antennas Propag.*, vol. 58, no. 3, pp. 690–696, Mar. 2010.

[19] P. Callaghan and E. A. Parker, "Experimental investigation of closely packed spiral element FSS yields narrowband designs," in *Proc. IEE ICAP91 Conf.*, 1991, pp. 636–639.

[20] B. A. Munk, R. G. Kouyoumjian, and L. Peters, "Reflection properties of periodic surfaces of loaded dipoles," *IEEE Trans. Antennas Propag.*, vol. AP-19, no. 5, pp. 612–617, Sep. 1971.

[21] [Online]. Available: http://www.shapeways.com/rrstatic/material_docs/msds-sandstone.pdf(accessed 08/05/2013)

[22] E. A. Parker and S. M. A. Hamdy, "Rings as elements for frequency selective surfaces," *Electron. Lett.*, vol. 17, pp. 612–614, 1981.

[23] S. M. A. Hamdy and E. A. Parker, "Current distribution on the elements of a square loop frequency selective surface," *Electron. Lett.*, vol. 18, pp. 624–626, 1982.

[24] A. D. Chuprin, E. A. Parker, and J. C. Batchelor, "Resonant frequencies of open and closed loop FSS arrays," *Electron. Lett.*, vol. 36, no. 19, pp. 1601–1603, Sep. 2000.

[25] B. A. Munk, *Frequency selective surfaces: theory and design*. New York, NY, USA: Wiley, 2000.

[26] A. H. Wong, M. J. Neve, and K. W. Sowerby, "Performance analysis for indoor wireless systems employing directional antennas in the presence of external interference," in *Proc. IEEE AP-S Int. Symp.*, Washington, DC, USA, 2005, vol. 1A, pp. 799–802.

Benito Sanz-Izquierdo received the B.Sc. degree from the University of Las Palmas de Gran Canaria, Las Palmas, Spain, and the M.Sc. and Ph.D. degrees from the University of Kent, Kent, U.K., in 2002 and 2007, respectively.

From 2003 to 2012, he was a Research Associate with the School of Engineering and Digital Arts, University of Kent, and in 2013, became a Lecture in electronic systems. In 2012, he spent some time working for Harada Industries, Ltd., where he developed novel antennas for the automotive industry. His research interests are multiband antennas, wearable microwave devices, substrate integrated waveguides components, electromagnetic band-gap structures, and frequency selective surfaces.

Edward A. (Ted) Parker received the M.A. degree in physics and the Ph.D. degree in radio astronomy from St. Catharine's College, Cambridge University, Cambridge, U.K.

He established the Antennas Group in the Electronics Laboratory at the University of Kent, Kent, U.K. The early work of that group focused on reflector antenna design, later on frequency selective surfaces and patch antennas. He was appointed Reader at the University of Kent in 1977, and since 1987 he has been Professor of Radio Communications, now Professor Emeritus.

Dr. Parker is a member of the IET.